RSC Advances

REVIEW

View Article Online
View Journal | View Issue

Cite this: *RSC Adv.*, 2023, **13**, 9665

MXene-based composites against antibiotic-resistant bacteria: current trends and future perspectives

Siavash Iravani *[a] and Rajender S. Varma [b]

Today, finding novel nanomaterial-based strategies to combat bacterial resistance is an important field of science. MXene-based composites have shown excellent antimicrobial potential owing to their fascinating properties such as excellent photothermal effects, highly active sites, large interlayer spacing, unique chemical structures, and hydrophilicity; they have great potential to damage the bacterial cells by rupturing the bacterial cell membranes, enhancing the permeability across the membrane, causing DNA damages, reducing the metabolic activity, and generating oxidative stress. After inserting into or attaching on the surface of pathogenic bacteria, these two-dimensional structures can cause bacterial membrane disruption and cell content leakage owing to their sharp edges. Remarkably, MXenes and their composites with excellent photothermal performance have been studied in photothermal antibacterial therapy to combat antibiotic-resistant bacteria and suppress chronic wound infections, thus providing new opportunities for multidrug-resistant bacteria-infected wound healing. But, details about the possible interactions between MXene-based nanosystems and bacterial cell membranes are rather scarce. Also, the mechanisms of photothermal antibacterial therapy as well as synergistic tactics including photothermal, photodynamic or chemo-photothermal therapy still need to be uncovered. This review endeavors to delineate critical issues pertaining to the application of MXene-based composites against antibiotic-resistant bacteria, focusing on their photocatalytic inactivation, physical damage, and photothermal antibacterial therapy.

Received 24th February 2023
Accepted 20th March 2023

DOI: 10.1039/d3ra01276j

rsc.li/rsc-advances

1. Introduction

Nowadays, a wide variety of two-dimensional (nano)structures such as graphene and its derivatives, layered double hydroxides, transition metal dichalcogenides, transition metal oxides, black phosphorus, graphitic carbon nitride, hexagonal boron nitride, boron nanosheets, and MXenes have been created for drug or gene delivery, imaging, biosensing, cancer therapy and diagnosis, antimicrobials, and tissue engineering.[1–5] These materials have shown unique physical, optical, biological, and chemical characteristics owing to their high surface-to-volume ratios, surface charge, and uniform architectures/shapes.[6–9] Among them, MXene-based composites have been intently designed with unique mechanical, thermal, optical, chemical, and electronic properties as advanced drug delivery systems, cancer nanotheranostic agents, tissue engineering materials, electrochemical capacitors, electromagnetic shielding materials, photocatalysts, and biosensors.[10–15] MXenes are a family of two-dimensional (2D) transition metal carbides, nitrides, and carbonitrides with a general formula of $M_{n+1}X_nT_x$, which were discovered in 2011 (the synthesis of Ti_3C_2) and are created from a bulk crystal termed MAX.[16,17] MXenes have hydrophilicity, inherently suitable conductivity, and great volumetric capacitance, as they comprise molecular sheets generated from the carbides and nitrides of transition metals like titanium. In addition to bare MXenes, the surfaces of MXenes can be terminated by functional groups bearing O, NH, S, Cl, Se, Br, and Te.[18] Both, the MXenes and graphene with large aspect ratio, active chemical surface, and varieties of fabrication techniques have shown excellent potential in flexible electronics, energy storage, and biomedical devices.[19,20] However, the exceptional electrical conductivity and electrochemical properties of MXenes render them promising candidates for flexible electronics and planar devices.[21,22] According to a study by Li *et al.*,[23] MXenes are intrinsically hydrophilic and have displayed higher electrical conductivity than solution processed graphene.

The spread of antibiotic-resistant bacteria necessitates the development of novel strategies to combat the acquired drug resistance and biofilm formation.[24–28] Since MXenes and their derivatives have exhibited suitable antimicrobial potentials with greatly reduced bacterial resistance (Table 1), they can be considered as promising alternatives for targeted antibacterial

[a]*Faculty of Pharmacy and Pharmaceutical Sciences, Isfahan University of Medical Sciences, 81746-73461, Isfahan, Iran. E-mail: siavashira@gmail.com*
[b]*Institute for Nanomaterials, Advanced Technologies and Innovation (CxI), Technical University of Liberec (TUL), Studentská 1402/2, Liberec 1 461 17, Czech Republic*

Table 1 Some selected studies on MXenes and their composites against pathogenic bacteria

MXene-based systems	Pathogenic bacteria	Strategies	Ref.
$Ti_3C_2T_x$	*E. coli*	Photocatalytic inactivation	43
$Ti_3C_2T_x$	*E. coli*	Photocatalytic inactivation	44
$Ag/Ti_3C_2T_x$	*E. coli* *Staphylococcus aureus*	Photothermal bactericidal effects	45
$Ti_3C_2T_x$	*E. coli* *Bacillus subtilis*	Damage to the bacterial cell membrane; oxidative stress	28
$Ti_3C_2T_x$	*E. coli* *B. subtilis*	Physical damages	46
$Ti_3C_2T_z$	*E. coli* *S. aureus*	Direct mechanical destruction	47
Nb_2CT_x; $Nb_4C_3T_x$	*E. coli* *S. aureus*	Physical damages; oxidative stress	48
Cu_2O/MXene	*S. aureus* *Pseudomonas aeruginosa*	Photocatalytic inactivation/ disinfection	49
$Ti_3C_2T_x$	*E. coli*	Outer membrane damages, causing cell growth inhibition	50
$Bi_2S_3/Ti_3C_2T_x$	*S. aureus* *E. coli*	Photo-excited killing of bacteria; photocatalytic inactivation	51
Ti_3C_2	Methicillin-resistant *S. aureus* vancomycin-resistant Enterococci	Photothermal ablation	52
MnO_2 and MoS_2 grown on Ti_3C_2 MXene	*E. coli* *B. subtilis*	Physical damages; changes of bacterial cell morphology; the main target was peptidoglycan mesh in bacterial cell walls	53
Ag_2S/Ti_3C_2	*S. aureus*	Synergistic photocatalytic and photothermal effects	54

drug delivery as well as non-invasive tactics to fight antibiotic-resistant bacteria.[29–32] These 2D structures could damage pathogenic bacteria *via* their sharp edges after insertion into and/or fastening on the surface of bacteria, thus realizing the bacterial membrane disruption and cell content leakage along with the chemical damages after the generation of oxidative stress or charge transfer.[33] Similar to graphene, MXenes exhibited suitable antibacterial effects against pathogenic bacteria in a dose dependent manner, but higher than those of graphene-based nanosystems.[28] MXene nanosheets with negatively charged surfaces and hydrophilicity had efficient bacterial contact to membrane surface, causing the microbial inactivation with direct contact-killing mechanisms.[34–39] Hydrogen bonding between oxygen-bearing groups of MXene-based materials and the lipopolysaccharide strings of the cell membrane may involve in the inhibition of bacteria *via* the avoidance of nutrient intake. But, details pertaining to the possible interactions between MXene-based nanosystems and bacterial cell membrane are still rather scarce.[28,38]

Photothermal therapy (PTT) is one of the innovative strategies with promising biomedical potential, especially for treating cancer. In this technique, nanomaterials are employed to convert light into heat energy to eliminate cancer cells.[40] Ongoing research aims to develop more effective photothermal agents with self-regulating photothermal conversion capability for selective obstructing cancer cells.[40] PTT using MXene-based composites under light irradiation can be considered as non-invasive alternative strategy to fight against bacterial proliferation. In this tactic, hyperthermia originating from the photo-to-thermal conversion process on the PTT agents entails the inactivation of proteins, cross-linking the deoxyribonucleic acid, and destroying the bacterial cell membranes, thus facilitating the penetration of antibacterial compounds to eliminate biofilm structures.[41] Such antibiotics-independent strategies have been applied for destroying pathogenic bacteria with efficient antibacterial effects and less light energy consumption.[41] In this context, combinational techniques such as PTT/photodynamic therapy (PDT) or chemo/PTT treatment of bacterial infections have shown synergistic antibacterial effects which can significantly improve the antibacterial efficiency, especially against antibiotic-resistant bacteria; the permeability of bacterial cell membranes can be enhanced by the heat generated *via* PTT, thus promoting the intracellular permeation of reactive oxygen species (ROS) or metal ions. In addition, by applying these synergistic strategies, the dosage requirements of photothermal agents or antibiotics are reduced, causing better elimination of pathogenic bacteria as well as reduction of possible side effects and improvement of therapeutic efficiency.[41,42]

Finding related antibacterial mechanisms can help to improve the functionality of MXenes as well as their inhibitory effects against antibiotic-resistant bacteria.[28] Several studies have focused on the physical damages of pathogenic bacteria through the disruption of cellular membranes as well as the chemical effects induced by oxidative stress and ROS formation.[55–58] However, non-invasive techniques such as PTT and photocatalytic inactivation using MXenes and their composites are still awaiting further exploration, especially

against antibiotic-resistant bacteria.[59] Since some pathogenic bacteria such as methicillin-resistant *S. aureus* exhibited resistance capabilities towards oxidant-based clearance pathways through the formation of antioxidants, the need to use novel techniques *via* the design of targeted antimicrobial drug delivery systems along with non-invasive strategies is felt more than ever.[59,60] Overall, the hybridization of MXenes with other organic and inorganic materials can result in materials with improved biocidal activities for versatile applications.[61] MXene nanosheets exhibited antimicrobial effects with direct mechanical destruction/physical damages, and can be considered as metal-based bactericides.[62] Recent advancements on photothermal conversion and antibacterial mechanisms pertaining to MXenes have been reported, as exemplified in the case of $Ti_3C_2T_x$ MXene with potent antibacterial activity against methicillin-resistant *S. aureus* (MRSA) and *E. coli.*[21,42] The design of novel MXene-based nanosystems with targeted antibacterial potentials can efficiently assist in controlling the bacterial infections along with elimination of bacterial resistance.[62] This review endeavored to delineate critical issues pertaining to the use of MXene-based composites against pathogenic and antibiotic-resistant bacteria, focusing on recent developments, important challenges, and future perspectives.

2. MXenes against antibiotic-resistant bacteria

2.1. Photocatalytic inactivation

MXenes have been applied for photocatalytic inactivation of antibiotic-resistant bacteria. For instance, TiO_2–MXene ($Ti_3C_2T_x$) nanohybrid was prepared as photocatalyst for the deactivation of *E. coli*[43] wherein this nanosystem exhibited photocatalytic activity (~30%) with inactivation of *E. coli* (~3.4 log order) under UV_{254} irradiation. The double membrane could protect bacteria from photocatalytic oxidation while high humidity could enhance the efficiency of photocatalytic inactivation *via* the formation of additional ROS.[43] In addition, MXenes ($Ti_3C_2T_x$) were applied in designing graphitic carbon-supported TiO_2 hybrid nanostructures for photocatalytic and bacteriostatic purposes.[44] Accordingly, these nanohybrid structures exhibited significant catalytic activity due to the formation of multiple interfacial junctions generated by graphitic carbon, TiO_2 nanoparticles, and MXenes, producing distinct intermediate energy levels for electron–hole pair separation and improving the catalytic performance. They illustrated high antibacterial effects (~97.4%) against *E. coli* under light exposure due to the free radicals generating oxidative stress on bacterial cells.[44] Li *et al.*[51] demonstrated that the photocatalytic performance of $Bi_2S_3/Ti_3C_2T_x$ could significantly enhance the amount of ROS under near-infrared (NIR) radiation (808 nm) to efficiently kill *S. aureus* (~99.86%) and of *E. coli* (~99.92%) with the assistance of hyperthermia within 10 min. This study reported the construction of an eco-friendly photo-responsive Schottky junction deploying MXenes to successfully eliminate bacterial infections.[51]

Photocatalysts comprising cuprous oxide (Cu_2O) were deployed with MXene nanosheets to show significant photocatalytic inactivation and synergistic antibacterial effects against *S. aureus* (~97.04%) and *P. aeruginosa* (~95.59%).[49] The electrons from Cu_2O were accepted by single-layer MXene with large surface area, forming abundant electrons on their surfaces to offer enhanced transfer of charge between bacterial cells and Cu_2O/MXene composites. MXene-based materials could stimulate the surface plasmon resonance enhancement to generate ROS on the surfaces of composites.[49] Furthermore, $Cu_2O/Ti_3C_2T_x$ nanosheets were designed for the elimination of multidrug resistant pathogenic bacteria (*e.g.*, methicillin-resistant *S. aureus*) from infected wound.[63] Accordingly, the Cu_2O could enhance generation of electron–hole pairs, boosting the photocatalytic formation of superoxide and ensuing transformation into hydrogen peroxide under NIR irradiation. Also, these nanosheets with sharp edges could directly damage bacterial cell membranes along with localized photothermal effects and generation of cytotoxic free radicals (*in situ*), displaying broad-spectrum antimicrobial activities.[63]

2.2. Photothermal, chemo-photothermal, and photodynamic therapy

PTT as quick and reliable technique has been deployed for combating antibiotic-resistant bacteria and suppressing bacterial infections without the development of drug resistance (Table 2);[64] however, limited studies have focused on synergistic PTT (with high temperature) and photodynamic therapy (with high level of ROS) against antibiotic-resistant bacteria. Photodynamic therapy is a two-stage treatment strategy that combines light energy with a drug (photosensitizer or photosensitizing agent) for biomedical applications, especially for treating cancer; the photosensitizer is activated by a specific wavelength of light energy, typically from a laser.[65] In one study, anisotropic MXene@polyvinyl alcohol hydrogels were constructed inspired by the hierarchical assembly of anisotropic structures across multiple length scales of muscles. The hydrogel not only endowed with excellent mechanical properties (stress up to 0.5 MPa and strain up to 800%) to be applied locally for hyperthermia of infected targets under NIR laser irradiation (808 nm), but also displayed significant antibacterial effects against *E. coli* (~98.3%) and *S. aureus* (~95.5%).[64] Owing to the excellent photothermal features of MXenes, the main antibacterial mechanism entailed hyperthermia and these hydrogels exhibited broad-spectrum antibacterial activities. These composites could efficiently promote the inhibition of wound infections and the healing process of skin wounds in mouse wound models (the rate of wound closure was ~98%); the hydrogels also effectively promoted the proliferation of NIH-3T3 cells. The results revealed that such MXene-based hydrogels with suitable toughness and anisotropy features can be deployed as potential antibacterial wound healing dressings.[64] In another study, MXene-based structures were designed for photothermal ablation of antibiotic-resistant bacteria,[42,52] with suitable antibacterial effects under NIR laser light irradiation within

Table 2 Some selected examples of PTT and photodynamic therapy strategies against antibiotic-resistant bacteria

MXenes	Strategies	Remarks	Ref.
$Ti_3C_2T_x$	Synergistic photothermal and photodynamic therapy	– The viability loss of methicillin-resistant *S. aureus* was significantly enhanced, including 45% for MXenes, 66% for indocyanine green, and 100% for indocyanine green–MXenes	67
V_2N	Photothermal effects with dual enzyme-like performances	– Significant anti-infective activity with excellent biocompatibility (*in vivo*) – Photo-enhanced nanozyme catalytic performances for the elimination of pathogenic bacteria and biofilms	68
Ti_3C_2	Photothermal-magnetolytic coupling antibacterial activities	– The photothermal conversion efficiency was ~48.7% – MXene-based composites (120 μg mL^{-1}) significantly eliminated *E. coli* and *S. aureus* (~100%)	69
Ti_3C_2	Photothermal antibacterial therapy and osteogenic potential	– High biocompatibility and bone formation capabilities – Excellent photothermal effects against both Gram-positive and Gram-negative bacteria	26
$Ti_3C_2T_x$	Photothermal effects along with physical destruction and light-enhanced enzymatic inactivation of methicillin-resistant *S. aureus*	– High light-to-heat conversion efficiency (~46.88%) – Wound disinfection (*in vivo*) with negligible biological toxicity	70
$Ti_3C_2T_x$	Photothermal effects; photothermally driven membrane distillation	– Robust interfacial interactions (hydrogen bonding) – Excellent porosity (>91%) with high mechanical stability	71
Ti_3C_2	Mild photothermal stimulation for diabetic wound healing	– Photothermal-controlled oxygen release MXene-based platforms – Improved antioxidant and antibacterial potential – Tissue adhesion, self-healing, injectability, and hemostasis – Applicability for infected diabetic wound healing	72
$Ti_3C_2T_x$	Photothermal antibacterial activity	– Effective killing of bacteria under NIR irradiation (808 nm) after 10 min – ~100% bacteriostasis rate; good cytocompatibility	73

~20 min. This technique could physically damage the structures of methicillin-resistant *S. aureus* and vancomycin-resistant Enterococci through direct contact and photothermal effects.[52] Antimicrobial activity of MXenes and their related composites (such as $Ti_3C_2T_x$ and Ag/$Ti_3C_2T_x$) could be highly boosted upon exposure to NIR light.[45] The synergistic antibacterial effects ensued because of photothermal bactericidal activities and physical damages which have been explored for wound dressings and against antibiotic-resistant bacteria (*E. coli* and *S. aureus*), with efficient display of wound healing after NIR laser light irradiation.[45] A combinational strategy was deployed for combating pathogenic bacteria using MXenes, gelatin methacrylate hydrogels, and bio-inert sulfonated polyether ether ketone.[66] Accordingly, the synergistic photothermal effects of MXenes and polydopamine could be applied for thermal ablation of the osteosarcoma cells under NIR irradiation; the efficient antibacterial effects could be attained against pathogenic bacteria after loading tobramycin drug. It appears that such photo-thermally controlled multifunctional platforms ought to be further studied, especially for cancer nanotherapy along with the treatment of bacterial infections.[66]

Anti-biofouling fibrous photothermal membranes with high flexibility comprising MXene-coated cellulose membrane have been prepared for highly efficient solar-driven water steam evaporation for water purification purposes.[74] These MXene/cellulose photothermal membranes exhibited high efficiency of light absorption (~94%) in a wide solar spectrum range with a water evaporation rate up to 1.44 kg m^{-2} h^{-1} under one solar illumination. These membranes with high antibacterial efficiency (~99.9%) are considered as promising bacteriostatic agents, which exhibited significant stability even under ultrasonication treatment and vigorous mechanical agitation owing to the sturdy interactions between MXenes and cellulose.[74] In addition, a NIR activated heterostructure catalyst was constructed from MXene (Ti_3C_2) and cobalt nanowires to perform against pathogenic bacteria based on synergistic NIR-stimulated ROS and hyperthermia (Fig. 1).[75] The photothermal effect could be highly strengthened owing to the synergy of plasmonic cobalt nanowires and MXenes. Accordingly, high antibacterial efficacy (>90%) was obtained against pathogenic bacteria within 20 min, showing efficient platforms with promising effects against antibiotic resistance. The mechanistic studies have illustrated that the electrons were stimulated upon the NIR laser illumination, from the valence band (VB) of MXene to its conduction band (CB). Afterward, the photogenerated electrons were transmitted to the surface of cobalt nanowires to react with oxygen to form ROS; some turned back to VB for recombination with holes *via* radiative transition, while the others returned to VB for recombination with holes *via* non-radiative transition. Besides, cobalt nanowires generated heat upon NIR irradiation, thus providing platforms with significantly improved photothermal property.[75]

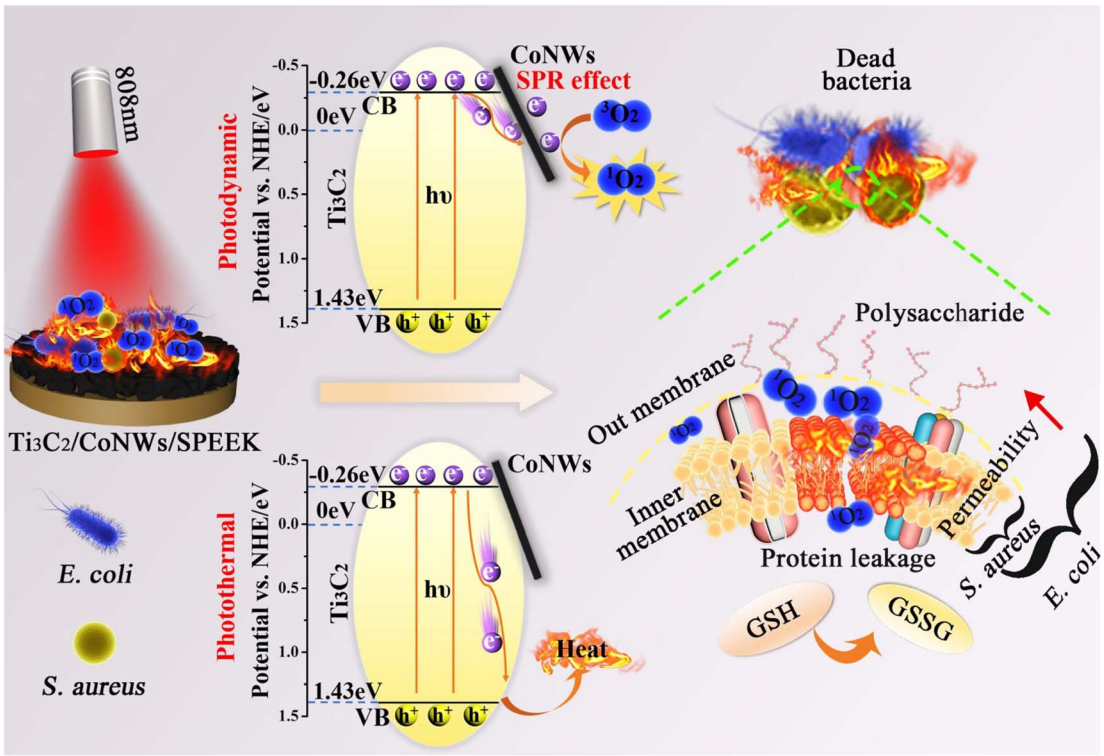

Fig. 1 The synergistic antibacterial mechanism for MXene/cobalt nanowires (CoNWs) with suitable photothermal property against pathogenic bacteria. SPEEK: sulfonated polyether ether ketone. Reproduced with permission from ref. 75 Copyright 2020 Elsevier.

Multimodal strategy for the control of bacterial infection was introduced by designing MXene (Nb_2C) nanosheets hybridized with medical implant of titanium plates for bacterial clearance and tissue regeneration applications. Accordingly, the platforms exhibited competent antibacterial effects by avoiding the generation of biofilms and preventing bacterial growth along with the stimulation of biofilm detachment (Fig. 2).[76] Mechanistic studies revealed that these composites could directly kill bacteria by down regulating the metabolism pathways, including tricarboxylic acid cycle and phosphotransferase system pathways. Besides, these MXene-based composites could sensitize bacteria towards hyperthermia and kill bacteria with NIR-responsive thermotherapy, thus paving a way for both bacterial/biofilm clearance and tissue remodeling; they could alleviate extra pro-inflammatory reactions and oxidative stress (*in vivo*), enhancing the angiogenesis and tissue remodeling procedure.[76]

Combinational chemo-PTT was introduced by deploying biocompatible MXene (Ti_3C_2) hybrid hydrogels with special membrane-disruption effects and high photo-thermal conversion efficiency under NIR light irradiation (Fig. 3).[77] Ciprofloxacin (an antibacterial drug) was combined with the MXene for the effective trap and killing of pathogenic bacteria; the release of ciprofloxacin was enhanced by NIR light irradiations to attain rapid and targeted ablation of bacteria. The excellent *in vitro* bactericidal efficiency of ~99.99% could be obtained for inhibiting methicillin-resistant *S. aureus* through the combinational chemo-PTT, providing nanosystems for efficient sterilization and long-term bacterial inhibition. However, the pre-/clinical studies along with the pharmacokinetics/pharmacodynamic evaluations ought to be undertaken by researchers to develop such systems for clinical applications (especially for chronic and diabetic wound healing).[77]

Size and morphology of MXene nanosheets are two crucial factors affecting their antibacterial effects. Gao *et al.*[78] evaluated the antibacterial PTT efficacy of MXene ($Ti_3C_2T_x$) nanosheets with size-dependent behavior against methicillin-resistant *S. aureus* (Fig. 4). Accordingly, by decreasing the size of MXene nanosheets, their antibacterial effects could be increased under NIR irradiation for 5 min. The size-dependent PTT efficacy of MXenes was comparable to that of the control antibacterial drug (vancomycin), offering new opportunities for the treatment of antibiotic-resistant bacteria infections.[78] Besides, MXene layers can significantly affect the antimicrobial properties. In one study, few- and multi-layer MXene ($Ti_3C_2T_x$) nanosheets were designed for PTT against *E. coli* and *S. aureus*,[79] wherein few-layer MXene nanosheets exhibited higher cytocompatibility and conversion of light to heat, while the multilayer nanosheets had a better efficacy towards the growth inhibition of pathogenic bacteria owing to the improved bacteria trapping capabilities. When multi-layer MXene nanosheets (100 μg mL^{-1}) were applied in combination with laser treatment at 5.7 W cm^{-2} (~5 min), the examined bacteria were completely eliminated; this strategy could provide an irreversible cell death linked to the loss of cell integrity, on the basis of results obtained from bacteria debris detection along with DNA release quantification studies.[79]

A composite membrane fabricated from titanium carbide (MXene), zeolite imidazole framework-8 (ZIF-8), and polylactic

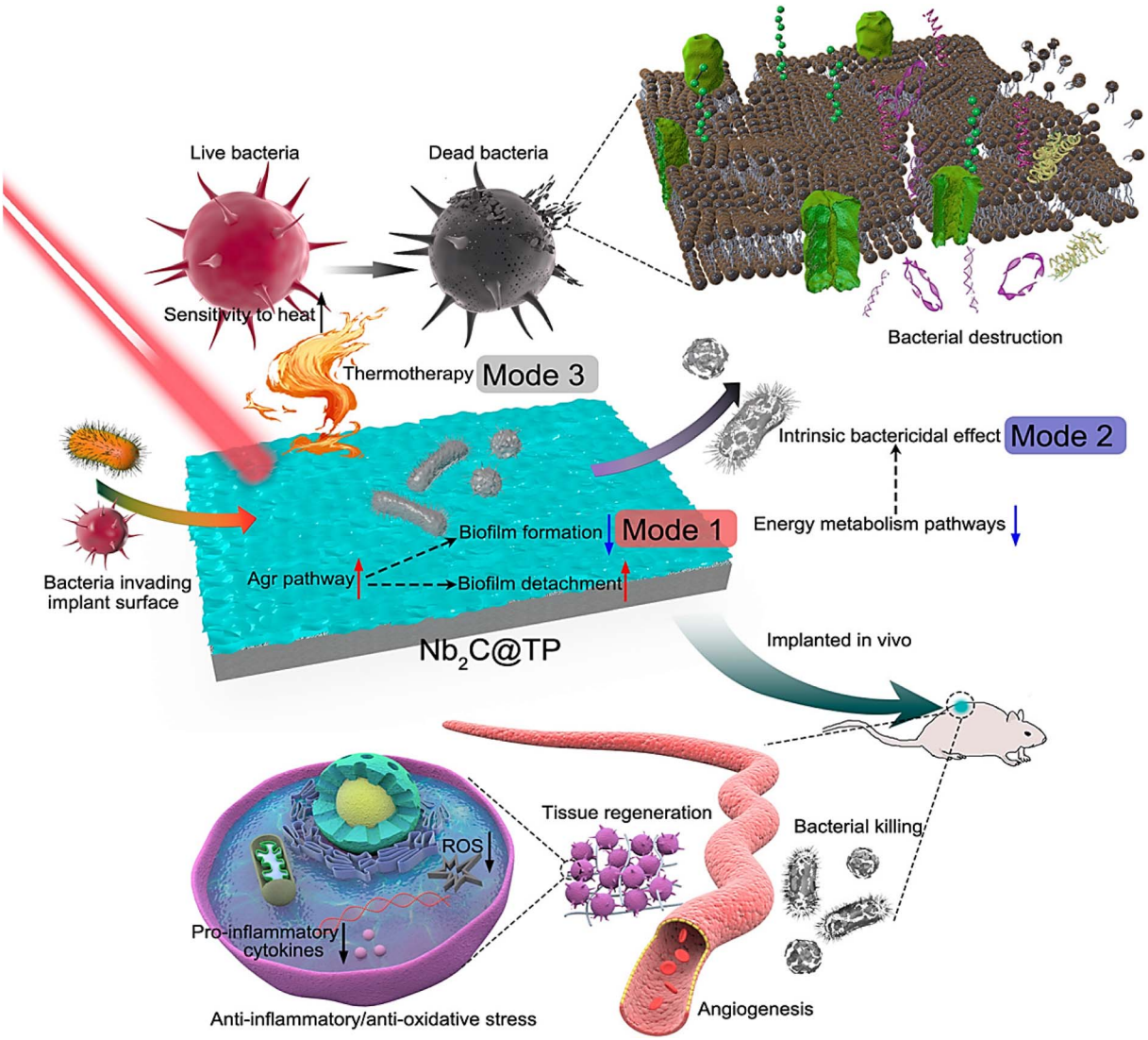

Fig. 2 MXene-based composites with bacterial killing effects, including biofilm resistant, intrinsic bactericidal, and thermo-ablation of bacteria strategies along with tissue regeneration features (*in vivo*). Reproduced with permission from ref. 76 Copyright 2020 American Chemical Society.

acid was introduced with the capability of generating singlet oxygen and hyperthermia (the photothermal convention efficiency was ~80.5%) against antibiotic resistant bacteria (the bactericidal rate was >99.0%).[80] The composite with efficient PTT and photodynamic therapy under laser irradiation (808 nm) displayed excellent antibacterial effects against *E. coli* (99.9%) and methicillin-resistant *S. aureus* (99.8%), thus providing an ideal platform against drug resistant bacterial infections and for wound healing without observable resistance (*in vivo*).[80] Fu *et al.*[81] constructed multifunctional biomass aerogels using $Ti_3C_2T_x$ (MXene) and silver nanowires on bacterial cellulose/chitosan composite aerogel by the deployment of physical mixture, lyophilization and electrostatic adsorption processes (Fig. 5). These composite aerogels were utilized as health monitoring sensor and antibacterial PTT. They exhibited robust photothermal conversion activity under NIR laser irradiation (808 nm), providing promising platforms with ~100% sterilizing effects owing to the synergistic antibacterial effects acquired from chitosan and silver nanowires along with the photothermal antibacterial effects of MXenes.[81]

2.3. Physical damages/inactivation and direct mechanical destruction

MXenes, specifically $Ti_3C_2T_x$, exhibited remarkable antibacterial effects through the physical damages and direct mechanical destruction of bacterial cells.[28] They disrupted the cellular membranes of bacteria leading to cell damage and eventual death. It has been reported that the antibacterial activities of MXenes were size- and exposure-time-dependent, and direct physical interactions between the sharp edges of MXene nanosheets and bacteria cells can play crucial roles in antibacterial features of these nanosheets.[46] Remarkably, hydrophilic MXene ($Ti_3C_2T_x$) coatings displayed suitable antibacterial activities against both *E. coli* and *B. subtilis*.[82] Nie

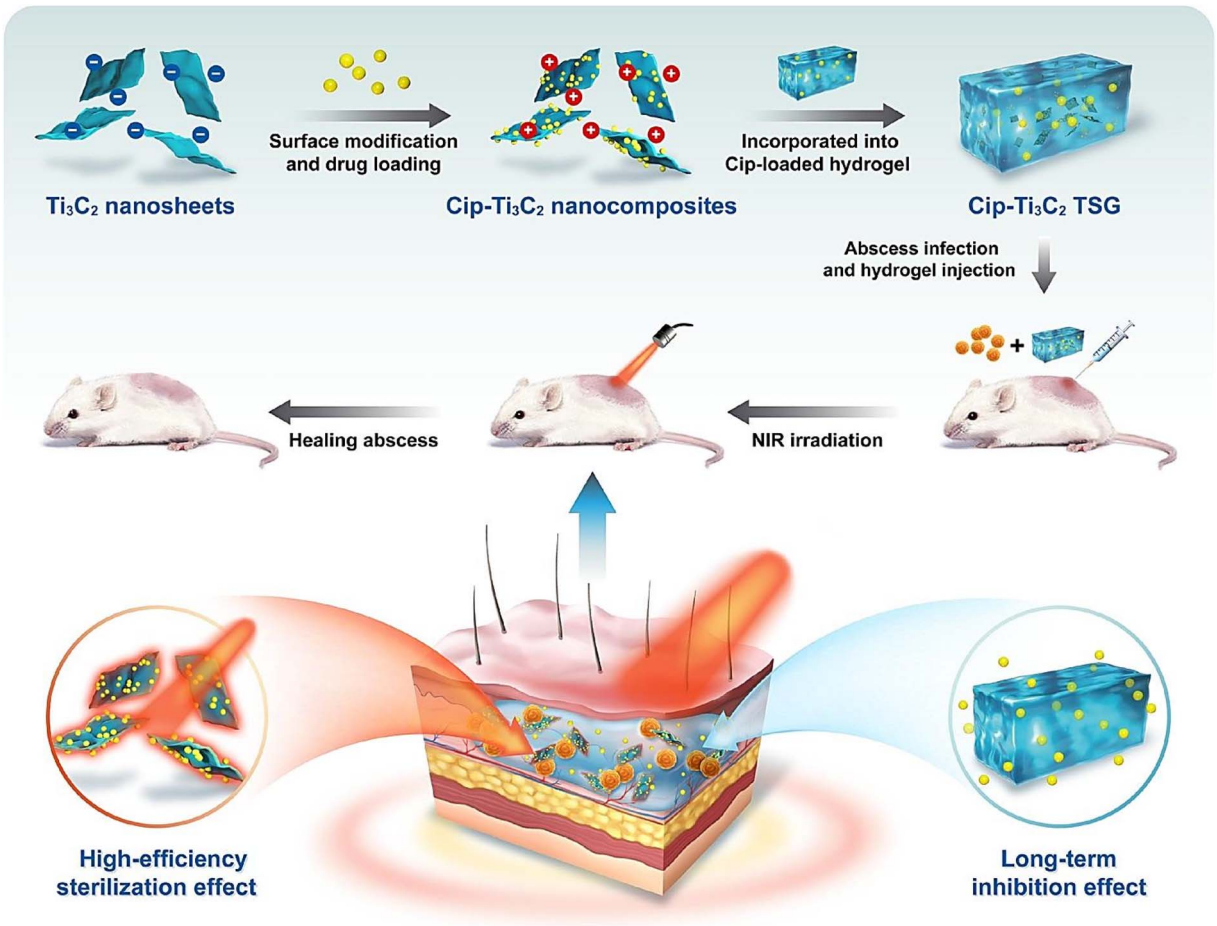

Fig. 3 MXene (Ti_3C_2) thermo-sensitive hydrogels (TSG) containing ciprofloxacin (Cip) for combinational chemo-phototherapy therapy against multidrug-resistant bacteria, paving a way for sterilization and long-term inhibition of pathogenic bacteria. Reproduced with permission from ref. 77 Copyright 2022 Elsevier.

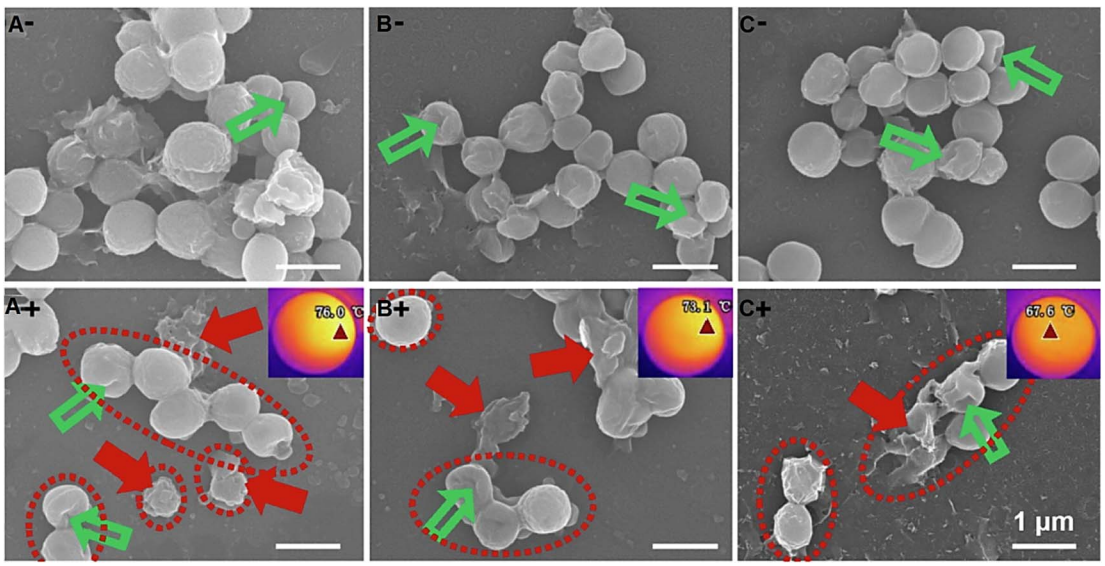

Fig. 4 (A–C) Scanning electron microscopy (SEM) images of methicillin-resistant *S. aureus* biofilm eradicated by MXenes. Scale bar = 1 μm. Green arrows indicate the dimples on cell surface; red arrows indicate the dead cells with significant morphology alterations; red dot circles indicate the separated methicillin-resistant *S. aureus* cells or clusters containing a few cells after biofilm broken; "−" and "+" represent no NIR and with NIR, respectively. Reproduced with permission from ref. 78 Copyright 2022 Elsevier.

et al. reported on the antibacterial properties of MXene-hybridized silane films, resulting in physical damages and direct mechanical destruction (Fig. 6).[27] In addition, MXenes ($Ti_3C_2T_x$) exhibited higher antibacterial effects against pathogenic bacteria compared to graphene oxide, showing concentration dependent bactericidal activities;[28] more than 98% bacterial cell viability loss could be detected at 200 μg mL^{-1} of MXenes for both bacterial cells after 4 h of exposure. These MXene-based structures physically damaged the bacterial cell membranes, causing the release of cytoplasmic materials from these cells. Also, the ROS dependent and independent stress stimulation has been reported.[28]

MXenes demonstrated appropriate antibacterial effects with lateral sizes of 0.09, 0.35, 0.57, and 4.40 μm against *E. coli* and *B.*

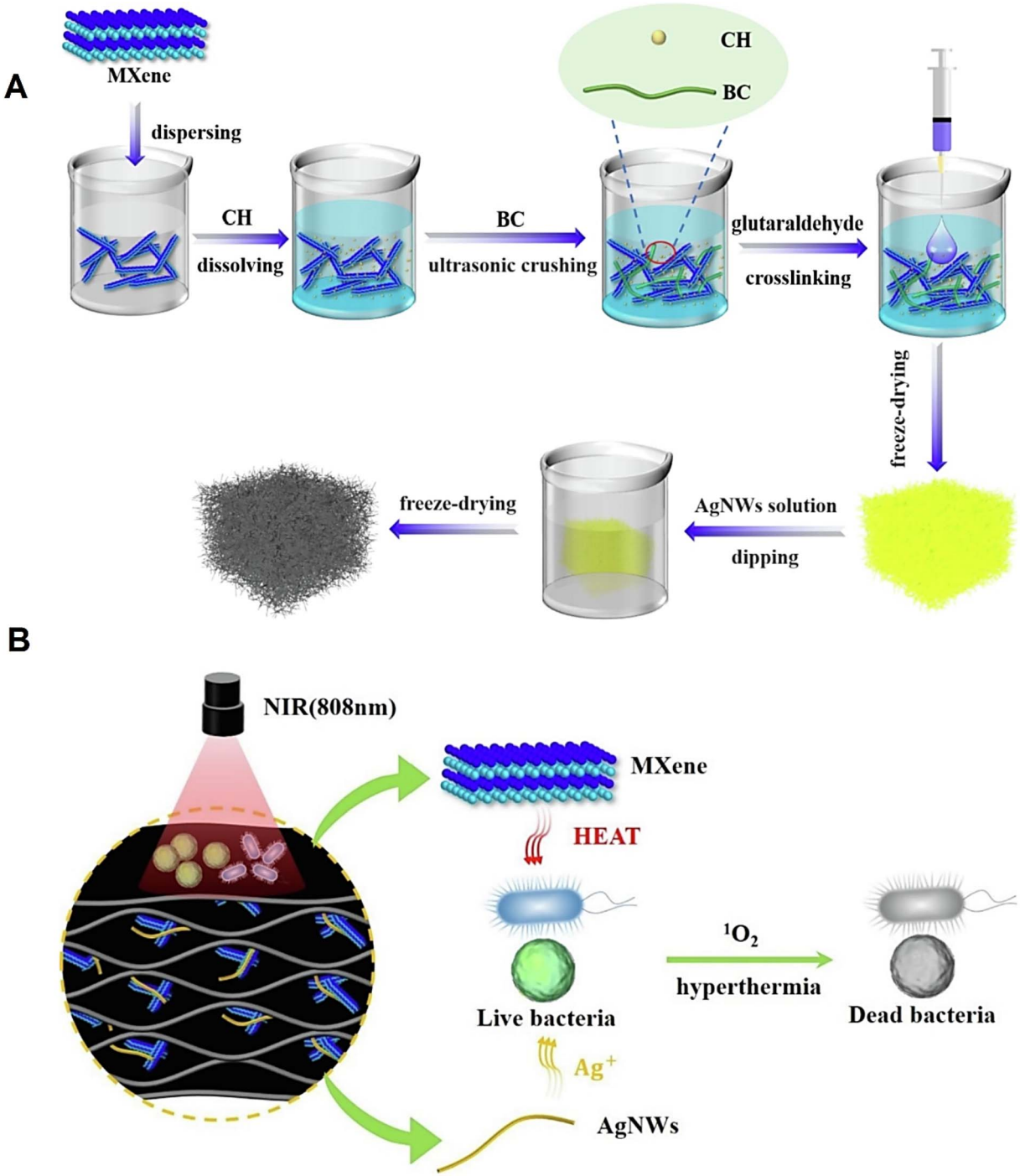

Fig. 5 (A) The preparative process of composite aerogel from bacterial cellulose (BC), chitosan (CH), MXene, and silver nanowires (AgNWs). (B) The antibacterial mechanisms of the composite aerogel against pathogenic bacteria. Reproduced with permission from ref. 81 Copyright 2022 Elsevier.

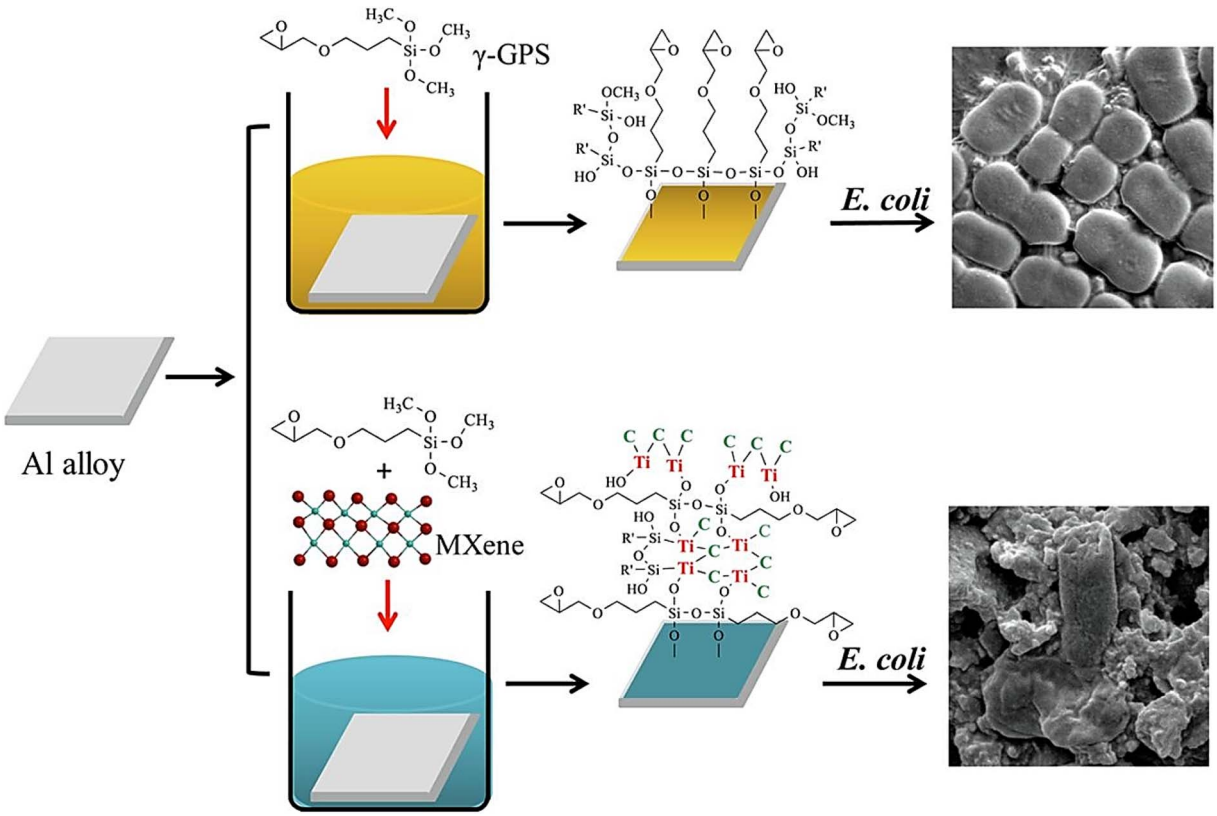

Fig. 6 MXene-hybridized silane films with antibacterial properties; MXene (Ti_3C_2) sheets were hybridized into the γ-glycidoxypropyltrimethoxysilane (γ-GPS) film on AA2024 aluminum (Al) alloy surface. Reproduced with permission from ref. 27 Copyright 2020 Elsevier.

subtilis for 3 and 8 h in the dark. Smaller nanosheets had higher antibacterial effects toward both the bacteria. Growth kinetics analyses evidently illustrated that direct physical interactions between the sharp edges of the nanosheets and bacteria membrane surfaces could play crucial roles in antibacterial properties, offering significant damages in bacterial cells in less than 3 h to release cellular contents followed by the dispersion of bacterial cells.[46] Overall, antibacterial effects of MXenes are influenced by atomic structures, morphologies, and sizes. In one study, MXenes (Nb_2CT_x and $Nb_4C_3T_x$) were analyzed for their antibacterial effects against resistant bacteria (*E. coli* and *S. aureus*).[48] Accordingly, the size of MXene sheets and their atomic structures could affect their antibacterial effects. After 3 h of incubation, Nb_2CT_x and $Nb_4C_3T_x$ demonstrated high growth inhibition of 94.2% and 96.1% for *E. coli* and 91.6 and 93.7% for *S. aureus*, respectively. By reducing the lateral sheet size of these MXenes, the viability of bacterial cells was also decreased; higher antibacterial effects could be obtained by smaller MXene nanosheets, which were related to their physical damages and oxidative stress mediated by them.[48] Zhou *et al.*[83] introduced $Ti_3C_2T_x$ (MXene)-based composite with high conductivity, biocompatibility, and antibacterial capabilities for methicillin-resistant *S. aureus*-infected wound healing applications (Fig. 7). Thus, the scaffolds with self-healing manner, electrical conductivity, tissue-adhesive property, antibacterial performance were obtained through the reactions among the poly(glycerol-ethylenimine), MXene@polydopamine nanosheets, and oxidized hyaluronic acid. The MXene@polydopamine composites disrupted the bacteria membranes, causing the leakage of proteins and eventual death. The outer membranous protuberances of methicillin-resistant *S. aureus*, membrane disruption, and leakage of cytoplasm contents could be detected.[83] The intracellular densities were significantly reduced by applying the MXene-based composites owing to the loss of some intracellular substance, indicating the membrane disruption and leakage of cytoplasmic contents. The designed MXene-based scaffolds could significantly enhance the wound healing by anti-inflammatory influences, stimulating the cell proliferation, angiogenesis, granulation tissue formation, collagen deposition, and vascular endothelial differentiation.[83]

MXene ($Ti_3C_2T_x$)-based membranes prepared by filtration on a polyvinylidene fluoride support were applied for damaging the surfaces of bacterial cells.[82] These membranes exhibited higher antibacterial effects against *B. subtilis* and *E. coli* compared to the control polyvinylidene fluoride samples; the flow cytometry evaluations illustrated ~70% population of dead and compromised cells after 24 h exposure of both bacterial strains to the membrane.[82] MXene-based membranes with excellent potentials against resistant bacteria should be further explored as anti-biofouling membranes in the wastewater treatment. For instance, membranes were constructed from MXenes ($Ti_3C_2T_x$) and silver nanoparticles for rapid water purification, showing excellent growth inhibition toward *E. coli* (~99%).[50] Physical and chemical damages could synergistically kill the bacteria

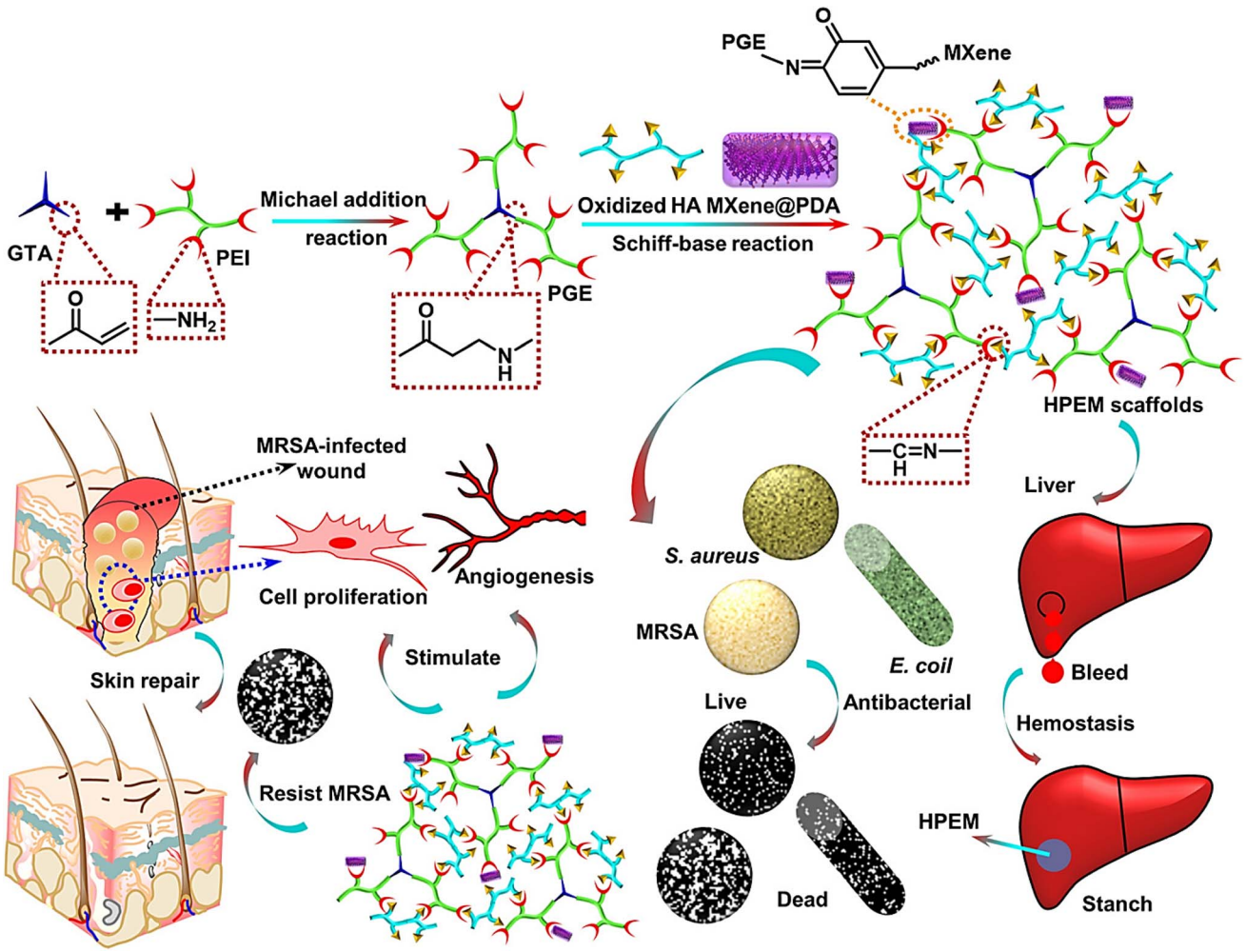

Fig. 7 The preparative process of multifunctional scaffolds (HPEM) for multidrug-resistant bacteria-infected wound healing purposes. MRSA: methicillin-resistant *S. aureus*; PDA: polydopamine; GTA: glycerol triacrylate; PGE: poly(glycerol-ethylenimine); PEI: polyethylenimine. Reproduced with permission from ref. 83 Copyright 2021 American Chemical Society.

and offer efficient antimicrobial effects. It was revealed that when ultra-small gold nanoclusters were conjugated on surfaces of MXene nanosheets, they could effectively transport into bacterial cells to produce localized ROS with high concentrations. In combination with physical damages ensued by MXene nanosheets, bacterial membrane lipids were efficiently oxidized and their membranes and DNAs were fragmented, offering synergistic antibacterial effects.[84] These nanosystems exhibited efficient bacterial death for both Gram-positive and Gram-negative bacteria, with low IC_{50} values of 11.7 μg mL^{-1} of MXene and 0.04 μm of gold nanomaterials. Notably, they obstructed the formation of biofilm due to the synergistic antibacterial effects, large surface area with higher density of bactericides, and hydrophobic surfaces avoiding the bacterial attachment.[84]

3. Challenges and perspectives

MXene-based composites have shown excellent potential in fighting antibiotic-resistant bacteria. The main mechanisms for deactivating bacteria by these composites include rupturing the bacterial membrane by sharp edges of MXenes nanoflakes and ROS generation as well as photothermal deactivation of bacteria.[28,41,61] Despite the developments in application of MXenes and their composites against pathogenic bacteria, their bactericidal mechanisms are still elusive. Studies have indicated that the adsorbed MXenes on membrane surfaces of bacteria could induce a local phase transition in a domain, and the leakage of intercellular molecules at the phase boundary could lead to defects and cell lysis.[85] In this context, several crucial parameters such as exposure time, size/morphology, thickness, concentration, epitaxy effects, exfoliation conditions, etching techniques/conditions, and surface charge/area can affect the antimicrobial effects of MXenes.[61]

There are some key challenges associated with MXenes, including their large-scale production, the cost of production and economic viability, stability issues, and environmental impacts/biosafety. Several studies have focused on improving the production strategies to produce them in more efficient manner and with cost-effectiveness, as exemplified in the case

of MXene fibers synthesized through a large-scale wet-spinning assembly.[86] For large-scale production of MXenes, sustainable and environmentally-friendly techniques ought to be further explored, avoiding the deployment of toxic and hazardous agents along with usage of complex or laborious steps/instrument.[29] Designing MXenes with specific morphologies requires taking into consideration a plethora of criteria that can affect their properties; scaling up the manufacturing of MXenes and their composites while preserving their quality and consistency necessitates more explorations.[87] On the other hand, the biosafety of MXenes/derivatives is an important consideration before their practical applications;[88] as with any new material, regulatory bodies need to assess their safety before they can be deployed in commercial products. Several tactics have been introduced for improving the biodegradability and biocompatibility of MXenes, including modification/hybridization techniques, fabrication of bioinspired structures, and greener synthesis.[89,90] For instance, a greener option has been reported for adjusting the potential cytotoxicity of MXenes after delamination by harnessing the interactions between the surface of MXene phases and collagen; surface modification with collagen could reduce the cytotoxicity of MXenes (*in vitro*) and their oxidative stress.[91]

Despite several advantages of MXenes such as hydrophilicity, electrical conductivity, flexibility, and pseudo-capacitance, they display poor stability under oxygen-containing circumstances owing to the presence of active transition metals, possible structural defects, and termination groups.[92,93] MXenes tend to degrade or undergo structural alterations when exposed to biological fluids, thereby affecting their performance and safety in biomedical applications; long-term stability of MXene-based materials with a minimal degradation rate is very important in designing clinical devices from them such as biosensors.[94,95] The as-prepared MXenes are typically in a thermodynamically metastable state and tend to react with trace oxygen or oxygen-containing molecules. Some techniques have been introduced for enhancing the stability of the as-obtained MXenes/derivatives by adjusting the storage conditions and generating shielding on the surface and/or edge of MXenes flakes.[96] Several studies have been organized to enhance the stability of MXenes/derivatives. One approach is to modify the surface of MXenes using additives such as polymers or surfactants.[96] Another strategy is to fabricate MXenes from MAX phases that have a higher oxidation resistance than their corresponding metals, as exemplified in the case of Al–Ti_3C_2 MXene with improved oxidation stability.[97] Zhang *et al.*[98] reported that the oxidation stability of colloidal MXene ($Ti_3C_2T_x$) aqueous solutions was better in argon (Ar) atmosphere at room temperature than in air atmosphere at low temperature, indicating the importance of atmosphere and temperature on the stability of MXenes.[98]

4. Conclusions

Today, with the indiscriminate use of antibiotics, bacterial resistance is increasing. Thus, the necessity of designing innovative nanosystems with targeted drug delivery capability and low side effects along with non-invasive treatments based on phototherapy for reducing bacterial resistance and effective treatment of resistant bacterial infections is felt more than before. In this context, combinational therapy and multi--mechanism antimicrobial agents with synergistic effects can efficiently combat antibiotic-resistant bacteria. Among the introduced materials, MXenes with high electrical conductivity, hydrophilicity, and unique optical/thermal features, as well as mechanical/electronic and tunable chemical properties can be considered as attractive candidates in designing novel micro- and nanosystems with antibacterial effects. MXene-based composites can physically damage bacterial membranes and chemically promote oxidative stress, showing high antimicrobial potentials for versatile environmental and biomedical applications. Remarkably, the strategies for the photocatalytic inactivation and photothermal ablation of antibiotic-resistant bacteria using MXene-based composites are still in their stage of infancy, demanding additional explorations. It appears that with developments in green chemistry-based synthesis strategies, future studies will move towards the simple, safer, and environmentally-benign fabrication of MXenes and their derivatives with high chemical stability and multifunctionality. Overall, the main and possible mechanisms for the deactivation or elimination of pathogenic bacteria by MXenes/derivatives include the rupture of bacterial cell membranes by sharp edges of MXenes nanoflakes, the inhibition of nutrient intake, the formation of ROS, and photothermal deactivation of bacteria. Finding the related antibacterial mechanisms along with the toxicological and pharmacological/pharmacokinetics studies can help to design next-generation MXene-based composites with high antibacterial effects.

Conflicts of interest

The author(s) declare no competing interest.

References

1 T. Hu, X. Mei, Y. Wang, X. Weng, R. Liang and M. Wei, *Sci. Bull.*, 2019, **64**, 1707–1727.
2 H. Huang, C. Dong, W. Feng, Y. Wang, B. Huang and Y. Chen, *Adv. Drug Delivery Rev.*, 2022, 114178, DOI: **10.1016/j.addr.2022.114178**.
3 K. Huang, Z. Li, J. Lin, G. Han and P. Huang, *Chem. Soc. Rev.*, 2018, **47**, 5109–5124.
4 S. K. Hwang, S.-M. Kang, M. Rethinasabapathy, C. Roh and Y. S. Huh, *Chem. Eng. J.*, 2020, **397**, 125428.
5 C. Murugan, V. Sharma, R. K. Murugan, G. Malaimegu and A. Sundaramurthy, *J. Controlled Release*, 2019, **299**, 1–20.
6 Z. Mohammadpour and K. Majidzadeh-A, *ACS Biomater. Sci. Eng.*, 2020, **6**, 1852–1873.
7 L. Wang, P. Hu, Y. Long, Z. Liu and X. He, *J. Mater. Chem. A*, 2017, **5**, 22855–22876.
8 Y. Wang, W. Feng and Y. Chen, *Chin. Chem. Lett.*, 2020, **31**, 937–946.
9 J. Zhu, G. S. Xiao and X. X. Zuo, *Nano-Micro Lett.*, 2020, **12**, 120.

10 Z.-K. Li, Y. Liu, L. Li, Y. Wei, J. Caro and H. Wang, *J. Membr. Sci.*, 2019, **592**, 117361.
11 H. Lin, Y. Chen and J. Shi, *Adv. Sci.*, 2018, **5**, 1800518.
12 H. Lin, S. Gao, C. Dai, Y. Chen and J. Shi, *J. Am. Chem. Soc.*, 2017, **139**, 16235–16247.
13 H. Lin, S. Gao, C. Dai, Y. Chen and J. Shi, *J. Am. Chem. Soc.*, 2017, **139**, 16235–16247.
14 H. Lin, X. Wang, L. Yu, Y. Chen and J. Shi, *Nano Lett.*, 2017, **17**, 384–391.
15 B. Fu, J. Sun, C. Wang, C. Shang, L. Xu, J. Li and H. Zhang, *Small*, 2021, **17**, 2006054.
16 Y. Gogotsi and Q. Huang, *ACS Nano*, 2021, **15**, 5775–5780.
17 M. Naguib, M. Kurtoglu, V. Presser, J. Lu, J. Niu, M. Heon, L. Hultman, Y. Gogotsi and M. W. Barsoum, *Adv. Mater.*, 2011, **23**, 4248–4253.
18 M. Tang, J. Li, Y. Wang, W. Han, S. Xu, M. Lu, W. Zhang and H. Li, *Symmetry*, 2022, **14**, 2232, DOI: **10.3390/sym14112232**.
19 R. Gautam, N. Marriwala and R. Devi, *Measurement: Sensors*, 2023, **25**, 100592.
20 Q. Song, F. Ye, L. Kong, Q. Shen, L. Han, L. Feng, G. Yu, Y. Pan and H. Li, *Adv. Funct. Mater.*, 2020, **30**, 2000475.
21 M. S. Salmi, U. Ahmed, N. Aslfattahi, S. Rahman, J. G. Hardy and A. Anwar, *RSC Adv.*, 2022, **12**, 33142–33155.
22 E. Mostafavi and S. Iravani, *Nano-Micro Lett.*, 2022, **14**, 130.
23 Y. Li, S. Huang, C. Wei, C. Wu and V. N. Mochalin, *Nat. Commun.*, 2019, **10**, 3014.
24 M. Mansoorianfar, K. Shahin, A. Hojjati-Najafabadi and R. Pei, *Chemosphere*, 2022, **290**, 133383.
25 E. A. Mayerberger, R. M. Street, R. M. McDaniel, M. W. Barsoum and C. L. Schauer, *RSC Adv.*, 2018, **8**, 35386–35394.
26 R. Nie, Y. Sun, H. Lv, M. Lu, H. Huangfu, Y. Li, Y. Zhang, D. Wang, L. Wang and Y. Zhou, *Nanoscale*, 2022, **14**, 8112–8129.
27 Y. Nie, J. Huang, S. Ma, Z. Li, Y. Shi, X. Yang, X. Fang, J. Zeng, P. Bi, J. Qi, S. Wang, Y. Xia, T. Jiao, D. Li and M. Cao, *Appl. Surf. Sci.*, 2020, **527**, 146915.
28 K. Rasool, M. Helal, A. Ali, C. E. Ren, Y. Gogotsi and K. A. Mahmoud, *ACS Nano*, 2016, **10**, 3674–3684.
29 S. Iravani, *Ceram. Int.*, 2022, **48**, 24144–24156.
30 S. Iravani and R. S. Varma, *Nanomaterials*, 2022, **12**, 1200.
31 G. Jamalipour Soufi, P. Iravani, A. Hekmatnia, E. Mostafavi, M. Khatami and S. Iravani, *Comments Inorg. Chem.*, 2022, **42**, 174–207.
32 M. Khazaei, A. Ranjbar, M. Arai, T. Sasaki and S. Yunoki, *J. Mater. Chem. C*, 2017, **5**, 2488–2503.
33 W. Sun and F.-G. Wu, *Chem.–Asian J.*, 2018, **13**, 3378–3410.
34 M. Khatami, H. Alijani and I. Sharifi, *IET Nanobiotechnol.*, 2018, **12**, 879–887.
35 M. Khatami, H. Q. Alijani, F. Mousazadeh, N. Hashemi, Z. Mahmoudi, S. Darijani, M. Bamorovat, A. Keyhani, M. Abdollahpour-Alitappehe and F. Borhani, *RSC Adv.*, 2020, **10**, 38063–38068.
36 M. Khatami, H. Q. Alijani, M. S. Nejad and R. S. Varma, *Appl. Sci.*, 2018, **8**, 411.
37 M. Khatami, S. Iravani, R. S. Varma, F. Mosazade, M. Darroudi and F. Borhani, *Bioprocess Biosyst. Eng.*, 2019, **42**, 2007–2014.
38 M. Khatami and S. Iravani, *Comments Inorg. Chem.*, 2021, **41**, 213–248.
39 E. Nazaripour, F. Mousazadeh, M. D. Moghadam, K. Najafi, F. Borhani, M. Sarani, M. Ghasemi, A. Rahdar, S. Iravani and M. Khatami, *Inorg. Chem. Commun.*, 2021, **131**, 108800.
40 L. Zhao, X. Zhang, X. Wang, X. Guan, W. Zhang and J. Ma, *J. Nanobiotechnol.*, 2021, **19**, 335.
41 M. Khatami, P. Iravani, G. Jamalipour Soufi and S. Iravani, *Mater. Technol.*, 2022, **37**, 1890–1905.
42 S. Hao, H. Han, Z. Yang, M. Chen, Y. Jiang, G. Lu, L. Dong, H. Wen, H. Li, J. Liu, L. Wu, Z. Wang and F. Wan, *Nano-Micro Lett.*, 2022, **14**, 178.
43 S. Lu, G. Meng, C. Wang and H. Chen, *Chem. Eng. J.*, 2021, **404**, 126526.
44 K. Rajavel, S. Shen, T. Ke and D. Lin, *Appl. Surf. Sci.*, 2021, **538**, 148083.
45 X. Zhu, Y. Zhu, K. Jia, B. S. Abraha, Y. Li, W. Peng, F. Zhang, X. Fan and L. Zhang, *Nanoscale*, 2020, **12**, 19129–19141.
46 A. A. Shamsabadi, M. Sharifian Gh, B. Anasori and M. Soroush, *ACS Sustainable Chem. Eng.*, 2018, **6**, 16586–16596.
47 E. A. Mayerberger, R. M. Street, R. M. McDaniel, M. W. Barsoum and C. L. Schauer, *RSC Adv.*, 2018, **8**, 35386–35394.
48 R. P. Pandey, P. A. Rasheed, T. Gomez, K. Rasool, J. Ponraj, K. Prenger, M. Naguib and K. A. Mahmoud, *ACS Appl. Nano Mater.*, 2020, **3**, 11372–11382.
49 W. Wang, H. Feng, J. Liu, M. Zhang, S. Liu, C. Feng and S. Chen, *Chem. Eng. J.*, 2020, **386**, 124116.
50 R. P. Pandey, K. Rasool, V. E. Madhavan, B. Aïssa, Y. Gogotsi and K. A. Mahmoud, *J. Mater. Chem. A*, 2018, **6**, 3522–3533.
51 J. Li, Z. Li, X. Liu, C. Li, Y. Zheng, K. W. K. Yeung, Z. Cui, Y. Liang, S. Zhu, W. Hu, Y. Qi, T. Zhang, X. Wang and S. Wu, *Nat. Commun.*, 2021, **12**, 1–10.
52 F. Wu, H. Zheng, W. Wang, Q. Wu, Q. Zhang, J. Guo, B. Pu, X. Shi, J. Li, X. Chen and W. Hong, *Sci. China Mater.*, 2021, **64**, 748–758.
53 F. Alimohammadi, M. Sharifian Gh, N. H. Attanayake, A. C. Thenuwara, Y. Gogotsi, B. Anasori and D. R. Strongin, *Langmuir*, 2018, **34**, 7192–7200.
54 Q. Wu, L. Tan, X. Liu, Z. Li, Y. Zhang, Y. Zheng, Y. Liang, Z. Cui, S. Zhu and S. Wu, *Appl. Catal., B*, 2021, **297**, 120500.
55 Y. Yang, J. Liu and X. Zhou, *Biosens. Bioelectron.*, 2021, **190**, 113418.
56 L. Xu, S. Jiang, J. Wu and Q. Zou, *Briefings Bioinf.*, 2021, **22**, bbaa171.
57 X.-F. Wang, P. Gao, Y.-F. Liu, H.-F. Li and F. Lu, *Curr. Bioinf.*, 2020, **15**, 493–502.
58 S. Sun, L. Xu, Q. Zou and G. Wang, *Bioinformatics*, 2021, **37**, 1319–1321.
59 X. Zou, L. Zhang, Z. Wang and Y. Luo, *J. Am. Chem. Soc.*, 2016, **138**, 2064–2077.

60 H. Enis Karahan, C. Wiraja, C. Xu, J. Wei, Y. Wang, L. Wang, F. Liu and Y. Chen, *Adv. Healthcare Mater.*, 2018, **7**, e1701406.
61 K. Salimiyan rizi, *J. Mol. Struct.*, 2022, **1262**, 132958.
62 F. Seidi, A. A. Shamsabadi, M. D. Firouzjaei, M. Elliott, M. R. Saeb, Y. Huang, C. Li, H. Xiao and B. Anasori, *Small*, 2023, 2206716, DOI: **10.1002/smll.202206716**.
63 Y.-J. Hsu, A. Nain, Y.-F. Lin, Y.-T. Tseng, Y.-J. Li, A. Sangili, P. Srivastava, H.-L. Yu, Y.-F. Huang, C.-C. Huang and H.-T. Chang, *J. Nanobiotechnol.*, 2022, **20**, 235.
64 Y. Li, M. Han, Y. Cai, B. Jiang, Y. Zhang, B. Yuan, F. Zhou and C. Cao, *Biomater. Sci.*, 2022, **10**, 1068–1082.
65 M. R. Hamblin and T. Hasan, *Photochem. Photobiol. Sci.*, 2004, **3**, 436–450.
66 J. Yin, Q. Han, J. Zhang, Y. Liu, X. Gan, K. Xie, L. Xie and Y. Deng, *ACS Appl. Mater. Interfaces*, 2020, **12**, 45891–45903.
67 C. Yu, S. Sui, X. Yu, W. Huang, Y. Wu, X. Zeng, Q. Chen, J. Wang and Q. Peng, *Colloids Surf., B*, 2022, **217**, 112663.
68 X. Sun, X. He, Y. Zhu, E. Obeng, B. Zeng, H. Deng, J. Shen and R. Hu, *Chem. Eng. J.*, 2023, **451**, 138985.
69 G. Liu, Q. Xiong, Y. Xu, Q. Fang, K. C.-F. Leung, M. Sang, S. Xuan and L. Hao, *Appl. Surf. Sci.*, 2022, **590**, 153125.
70 D. Zhang, L. Huang, D.-W. Sun, H. Pu and Q. Wei, *Chem. Eng. J.*, 2023, **452**, 139078.
71 S. Cao, X. Wu, Y. Zhu, P. Gupta, A. Martinez, Y. Zhang, D. Ghim, Y. Wang, L. Liu, Y.-S. Jun and S. Singamaneni, *J. Mater. Chem. A*, 2021, **9**, 22585–22596.
72 Y. Li, R. Fu, Z. Duan, C. Zhu and D. Fan, *ACS Nano*, 2022, **16**, 7486–7502.
73 T. Du, S. Zhao, W. Dong, W. Ma, X. Zhou, Y. Wang and M. Zhang, *ACS Biomater. Sci. Eng.*, 2022, **8**, 2375–2389.
74 X.-J. Zha, X. Zhao, J.-H. Pu, L.-S. Tang, K. Ke, R.-Y. Bao, L. Bai, Z.-Y. Liu, M.-B. Yang and W. Yang, *ACS Appl. Mater. Interfaces*, 2019, **11**, 36589–36597.
75 Y. Liu, Y. Tian, Q. Han, J. Yin, J. Zhang, Y. Yu, W. Yang and Y. Deng, *Chem. Eng. J.*, 2021, **410**, 128209.
76 C. Yang, Y. Luo, H. Lin, M. Ge, J. Shi and X. Zhang, *ACS Nano*, 2021, **15**, 1086–1099.
77 Y. Zheng, Y. Yan, L. Lin, Q. He, H. Hu, R. Luo, D. Xian, J. Wu, Y. Shi, F. Zeng, C. Wu, G. Quan and C. Lu, *Acta Biomater.*, 2022, **142**, 113–123.
78 Y. Gao, Y. Dong, S. Yang, A. Mo, X. Zeng, Q. Chen and Q. Peng, *J. Colloid Interface Sci.*, 2022, **617**, 533–541.
79 A. Rosenkranz, G. Perini, J. Y. Aguilar-Hurtado, D. F. Zambrano, B. Wang, B. Niccolini, P. C. Henriques, E. Rosa, F. D. Maio, G. Delogu, M. D. Spirito, V. Palmieri and M. Papi, *Appl. Surf. Sci.*, 2021, **567**, 150795.
80 S. Zhang, J. Ye, X. Liu, Y. Wang, C. Li, J. Fang, B. Chang, Y. Qi, Y. Li and G. Ning, *J. Colloid Interface Sci.*, 2021, **599**, 390–403.
81 Y. Fu, Y. Cheng, Q. Wei, Y. Zhao, W. Zhang, Y. Yang and D. Li, *Appl. Surf. Sci.*, 2022, **598**, 153783.
82 K. Rasool, K. A. Mahmoud, D. J. Johnson, M. Helal, G. R. Berdiyorov and Y. Gogotsi, *Sci. Rep.*, 2017, **7**, 1598.
83 L. Zhou, H. Zheng, Z. Liu, S. Wang, Z. Liu, F. Chen, H. Zhang, J. Kong, F. Zhou and Q. Zhang, *ACS Nano*, 2021, **15**, 2468–2480.
84 K. Zheng, S. Li, L. Jing, P. Y. Chen and J. Xie, *Adv. Healthcare Mater.*, 2020, **9**, 2001007.
85 O.-S. Lee, M. E. Madjet and K. A. Mahmoud, *Nano Lett.*, 2021, **21**, 8510–8517.
86 W. Eom, H. Shin, R. B. Ambade, S. H. Lee, K. H. Lee, D. J. Kang and T. H. Han, *Nat. Commun.*, 2020, **11**, 2825.
87 C. E. Shuck, A. Sarycheva, M. Anayee, A. Levitt, Y. Zhu, S. Uzun, V. Balitskiy, V. Zahorodna, O. Gogotsi and Y. Gogotsi, *Adv. Eng. Mater.*, 2020, **22**, 1901241.
88 A. Zamhuri, G. P. Lim, N. L. Ma, K. S. Tee and C. F. Soon, *BioMed. Eng. OnLine*, 2021, **20**, 1–24.
89 H. Li, R. Fan, B. Zou, J. Yan, Q. Shi and G. Guo, *J. Nanobiotechnol.*, 2023, **21**, 73, DOI: **10.1186/s12951-12023-01809-12952**.
90 S. Iravani and R. S. Varma, *Mater. Adv.*, 2022, **3**, 4783–4796.
91 A. Rozmysłowska-Wojciechowska, A. Szuplewska, T. Wojciechowski, S. Poźniak, J. Mitrzak, M. Chudy, W. Ziemkowska, L. Chlubny, A. Olszyna and A. M. Jastrzębska, *Mater. Sci. Eng., C*, 2020, **111**, 110790.
92 Z. Zheng, C. Guo, E. Wang, Z. He, T. Liang, T. Yang and X. Hou, *Inorg. Chem. Front.*, 2021, **8**, 2164–2182.
93 W. Meng, X. Liu, H. Song, Y. Xie, X. Shi, M. Dargusch, Z.-G. Chen, Z. Tang and S. Lu, *Nano Today*, 2021, **40**, 101273.
94 Z. U. D. Babar, B. D. Ventura, R. Velotta and V. Iannotti, *RSC Adv.*, 2022, **12**, 19590–19610.
95 A. Hermawan, T. Amrillah, A. Riapanitra, W.-J. Ong and S. Yin, *Adv. Healthcare Mater.*, 2021, **10**, 2100970.
96 J. Jiang, S. Bai, J. Zou, S. Liu, J.-P. Hsu, N. Li, G. Zhu, Z. Zhuang, Q. Kang and Y. Zhang, *Nano Res.*, 2022, **15**, 6551–6567.
97 A. Iqbal, J. Hong, T. Y. Ko and C. M. Koo, *Nano Convergence*, 2021, **8**, 1–24.
98 C. J. Zhang, S. Pinilla, N. McEvoy, C. P. Cullen, B. Anasori, E. Long, S.-H. Park, A. Seral-Ascaso, A. Shmeliov, D. Krishnan, C. Morant, X. Liu, G. S. Duesberg, Y. Gogotsi and V. Nicolosi, *Chem. Mater.*, 2017, **29**, 4848–4856.